



The Spectrum of CT Findings of COVID-19 Pneumonia: Acute Alveolar Insult and Organizing Pneumonia as Different Phases of Lung Injury and Repair

COVID-19 폐렴의 다양한 CT 영상 소견: 급성 폐포 손상과 기질화 폐렴

Yun Su Kim, MD , Ung Rae Kang, MD* , Young Hwan Kim, MD

Department of Radiology, Daegu Catholic University Medical Center, Catholic University of Daegu College of Medicine, Daegu, Korea

Purpose To analyze the findings and serial changes in chest CT lesions in 123 symptomatic patients with coronavirus disease 2019 (COVID-19).

Materials and Methods From February 19 to April 7, 2020, a total of 123 confirmed COVID-19 patients (male, 44; female, 79; mean age, 59.2 ± 18.6) were enrolled in this retrospective study. A total of 234 CT scans were reviewed for the following patterns: acute alveolar insult (AAI) patterns: ground-glass opacity (GGO), crazy-paving appearance, mixed pattern, and consolidation; organizing pneumonia (OP) patterns: perilobular patterns, band opacity, curvilinear opacity, reversed halo opacity, and small nodular consolidation; resolving patterns: pure GGO, remnant curvilinear, small nodular consolidation, and serial changes of lung abnormalities. We compared the proportions of AAI pattern, OP pattern, or resolving pattern with time progression and analyzed the association between the patterns and disease severity using Pearson chi-square and Fisher's exact test.

Results Predominant CT patterns were AAI pattern (87%) in the early hospital period group (0-10 days, after the onset of symptoms), OP pattern (45.7%) in the later hospital period group (after 10 days), and resolving pattern in discharge and follow-up group (47.2% and 84.8%, respectively). The difference in the proportions of predominant CT patterns with time progression was statistically significant ($p < 0.001$, Pearson's chi-square test). No statistically significant association was observed between the patterns and disease severity ($p = 0.055$, Fisher's exact test). No fibrous changes in the lesions were observed on follow-up CT scans.

Conclusion The serial CT scans of COVID-19 patients showed the spectrum of COVID pneumonia CT manifestations as different phases of lung injury and repair.

Received July 28, 2020
Revised October 31, 2020
Accepted December 9, 2020

*Corresponding author

Ung Rae Kang, MD
Department of Radiology,
Daegu Catholic University
Medical Center,
Catholic University
of Daegu College of Medicine,
33 Duryugongwon-ro 17-gil,
Nam-gu, Daegu 42472, Korea.

Tel 82-53-650-4328
Fax 82-53-650-4339
E-mail urkang@cu.ac.kr

This is an Open Access article distributed under the terms of the Creative Commons Attribution Non-Commercial License (<https://creativecommons.org/licenses/by-nc/4.0>) which permits unrestricted non-commercial use, distribution, and reproduction in any medium, provided the original work is properly cited.

ORCID iDs

Yun Su Kim
[https://
orcid.org/0000-0003-1542-6189](https://orcid.org/0000-0003-1542-6189)
Ung Rae Kang
[https://
orcid.org/0000-0002-4420-4836](https://orcid.org/0000-0002-4420-4836)
Young Hwan Kim
[https://
orcid.org/0000-0002-2545-6923](https://orcid.org/0000-0002-2545-6923)

Index terms Computed Tomography, X-Ray; COVID-19; Acute Lung Injury; Pneumonia

INTRODUCTION

An outbreak of unknown viral pneumonia was first reported in Wuhan, China in December 2019, and its etiology was defined as the novel coronavirus (SARS-CoV-2) and termed coronavirus disease 2019 (COVID-19) (1). As of May 28, 2020, the disease has rapidly spread and progressed worldwide, with approximately 5500000 patients. An outbreak of COVID-19 also developed in Daegu, Korea in early February 2020. Daegu city emerged as the hotbed of coronavirus outbreaks in Korea, along with neighboring North Gyeongsang Province. A recently published pathologic study on COVID-19 pneumonia revealed diffuse alveolar damage (DAD) and organizing pneumonia (OP) as histologic findings (2). Zhang et al. (3) also showed histopathological findings such as DAD and organization by their lung biopsy examination for lesions showing GGO on CT results of COVID-19 patients. The real-time reverse transcriptase-polymerase chain reaction (RT-PCR) method with nose and throat swabs is the most reliable tool to confirm COVID-19 (4). However, this method has limitations, which do not provide any information about the disease severity of pneumonia. Chest CT scanning can evaluate the patients for screening and assessing disease severity and the present state of disease. A chest CT study can evaluate acute lung injury (ALI) as consolidation and ground-glass opacity (GGO) with gravitationally gradient, more consolidative lesions in the posterobasal area of the lungs, or crazy-paving pattern (5). In addition, several CT features of OP have been reported, including band opacity, perilobular consolidation or GGO, or small nodular consolidation (6-9). In this study, we evaluated the characteristics and interval changes of CT findings from COVID-19 patients in order to explain CT findings and the present state of lesions.

MATERIALS AND METHODS

We received research approval from the Institutional Review Board. Because of the retrospective nature of the study, informed consent was not required (IRB No. CR-20-127-L).

PATIENTS

This retrospective study enrolled 123 patients (male, 44; female, 79; mean age, 59.2 ± 18.6) who were admitted from February 19 to April 7, 2020, with confirmed COVID-19 by RT-PCR, and classified as moderate severity according to the Korea Centers for Disease Control and Prevention (KCDC) guidelines. The KCDC had provided guidelines (7th edition) that allocated hospital beds to patients according to the following classification for disease severity (10): 1) no symptom: patients presenting all following items: a. consciousness; b. age < 50 years; c. no underlying disease; d. non-smoker; e. body temperature < 37.5°C without taking antipyretics; 2) mild: conscious patients with any one of the following: a. age < 50 years; b. one or more underlying disease; c. fever $\leq 38^\circ\text{C}$ and taking antipyretics; 3) moderate: conscious patients with one or more of the following: a. fever > 38°C despite taking antipyretics; b. dys-

nea; 4) severe: unconscious patients. Patients showed fever $> 38^{\circ}\text{C}$ despite taking antipyretics ($n = 64, 52.0\%$) or dyspnea ($n = 52, 42.3\%$) at admission.

CT SCANNING

Either of the two equipment was scanned for chest CT (Revolution CT, GE Healthcare, Milwaukee, WI, USA; Somatom Definition Flash, Siemens Healthineers, Forchheim, Germany). The CT parameters were as follows: tube voltage, 100 kVp (kV assist); tube current, 80–400 mAs (smart mA); detector collimation, 2.5 mm; and beam pitch, 0.992. The CT scans for contrast-enhancement were obtained after 40 s of injection with nonionic iodinated contrast media of 80–90 mL (Optiray 350, Liebel-Flarsheim, Quebec, Canada) at a rate of 2 mL/s using a power injector (Bayer Medical care; Medrad, Pittsburgh, PA, USA). The acquired data were reconstructed in 1.25–2.5 mm thickness using a lung algorithm.

CT IMAGE ANALYSIS

Attending radiologists of two groups (group one: one radiologist with a 20-year experience in radiology; group two: two radiologists with 10- and 3-year radiology experience) independently reviewed the CT images on a picture archiving and communication system (PACS, INFINTT Healthcare Co., Ltd., Seoul, Korea). The CT images were assessed for the presence of GGO, crazy-paving appearance (GGO with septal thickening), mixed opacity (combination of GGO and consolidation), consolidation, band opacity (thick radial bands of consolidation), peribulbar consolidation (arcade-like consolidation distributed along the secondary pulmonary lobule), peribulbar GGO (arcade-like GGO distributed along the secondary pulmonary lobule), small nodular consolidation (ill-defined GGO nodular consolidation with peribronchial distribution), and thin curvilinear opacity (Figs. 1, 2). The CT abnormalities were classified into four groups: 1) acute alveolar insult (AAI) patterns: ALI and suspicious acute alveolar wall damage, CT findings showing GGO, crazy-paving appearance, mixed opacity, and consolidation; 2) transition pattern: CT findings mixed with AAI and OP pattern; 3) OP patterns: proposed as having organization, CT findings showing band opacity, peribulbar patterns, and small nodular consolidation; 4) resolving patterns: proposed as recovery state having remnant lesions with decreased extent, CT findings showing remnant small nodular consolidation, remnant peribulbar GGO, pure GGO, and thin curvilinear opacity. The radiologists of the two groups reached a consensus for differences in image-finding assessments.

DEFINITION OF CLASSIFICATIONS

The CT scans were classified into four groups based on the elapsed period from symptom onset to CT examination: 1) early hospital period group: period between symptom onset and CT scanning ≤ 10 days; 2) later hospital period group: period > 10 days; 3) discharge group: CT scanning at the time of discharge; 4) follow-up group: CT scanning for a follow-up check after discharge.

Admitted patients were re-classified into four groups according to severity (11): 1) mild group: patients with fever $> 38^{\circ}\text{C}$, mild dyspnea, and normal CT findings; 2) moderate group: patients with fever $> 38^{\circ}\text{C}$, moderate dyspnea, and showing CT lesions; 3) severe group: patients with any one of the following: respiratory distress, respiratory rate $\geq 30/\text{min}$; b. oxygen

saturation $\leq 93\%$ in resting condition; c. arterial partial pressure of oxygen (PaO₂) /oxygen concentration (FiO₂) ≤ 300 mm Hg; 4) very severe group: patients with any one of the following: a. respiratory failure requiring mechanical ventilation; b. shock; c. requiring intensive care unit (ICU) admission.

STATISTICAL ANALYSIS

We analyzed the proportions of AAI pattern, OP pattern, and resolving pattern with time progression using Pearson chi-square and Fisher's exact tests. The association between the patterns and disease severity was also analyzed using Fisher's exact test. The statistical analysis was performed with the software of SPSS (version 22.0; IBM Corp., Armonk, NY, USA). The variables showing *p* values < 0.05 were considered statistically significant.

RESULTS

PATIENTS

During the study period, a total of 123 consecutive patients confirmed with COVID-19 by RT-PCR and classified as having moderate severity according to the KCDC guidelines were admitted to the isolation ward. The median illness duration from symptom to confirmation was 3 days (range: 0–39 days). The mean hospitalization duration was 29 days (range, 2–65). Nine patients (7.3%) died during hospitalization. Reactivation of COVID-19 after discharge occurred in seven patients (6.1%). The clinical symptoms were fever in 64 patients, dyspnea in 52 patients, cough in 42 patients, sputum in 12 patients, rhinorrhea in four patients, and fatigue in two patients. According to the in-hospital severity classification, the admitted patients were classified as mild ($n = 62$, 50%), moderate ($n = 35$, 29%), severe ($n = 14$, 11%), and very severe ($n = 12$, 10%). Among the 123 patients, 91 (74%) had underlying diseases, such as hypertension ($n = 36$), diabetes mellitus ($n = 29$), cerebral infarction ($n = 18$), cardiovascular disease ($n = 12$), pulmonary tuberculosis (TB) ($n = 11$), chronic renal insufficiency ($n = 10$), chronic liver disease ($n = 8$), asthma ($n = 8$), emphysema ($n = 4$), congestive heart failure ($n = 4$), cerebral hemorrhage ($n = 1$), and lung abscess ($n = 1$). The demographics and baseline characteristics of the patients are summarized in Table 1.

A total of 234 chest CT scans were acquired for the study, 93 scans during hospitalization, 108 scans at discharge, and 33 scans for follow-up after discharge. Days from symptom onset to CT scan during hospitalization, at discharge, and for the follow-up study were 16.6 ± 9.0 , 33.3 ± 14.1 , and 67.2 ± 14.3 , respectively.

CHEST CT FINDINGS

The study noticed no obvious abnormality on chest CT in three CT scans (13%) in the early hospital period group, 15 scans (21%) in the later hospital group, 37 scans (34%) in the discharge group, and three scans (9%) in the follow-up group. CT scans were obtained for five of the nine fatal cases. One patient showed an acute respiratory distress syndrome (ARDS) pattern with anterior-posterior gradient distribution, two patients showed diffuse consolidation, and one patient showed a diffuse crazy-paving appearance. In the early hospital group, pure GGO, crazy-paving appearance, mixed opacity, or consolidation were predominantly ob-

Table 1. Demographics and Baseline Characteristics of Patients (n = 123)

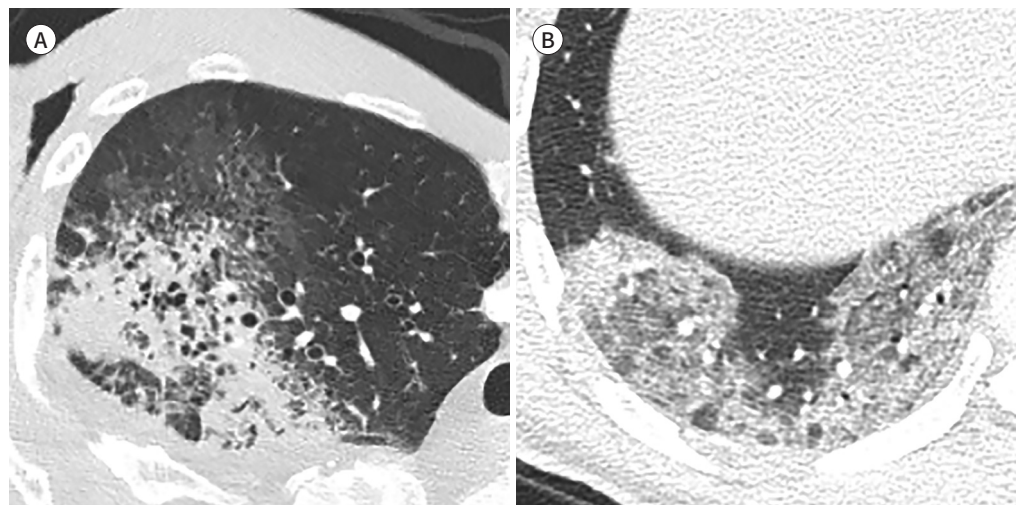
Characteristics	Findings
Sex (male/female)	44/79
Ages (years)	59.2 ± 18.6
Symptoms	
Fever	64 (52.0)
Cough	42 (34.1)
Sputum	12 (9.8)
Rhinorrhea	4 (3.3)
Fatigue	2 (1.6)
Dyspnea	52 (42.3)
Other symptoms	7 (5.7)
Severity of patients	
Mild	62 (50.3)
Moderate	35 (28.5)
Severe	14 (11.4)
Very severe	12 (9.8)
Days from symptoms onset to CT scan	16.6 ± 9.0
Days from symptoms onset to discharge scan	33.3 ± 14.1
Days from symptoms onset to follow-up scan	67.2 ± 14.3
Underlying disease	91 (74)
Clinical outcomes	
Discharge	114 (92.7)
Fatal	9 (7.3)
Reactivation after discharge	7 (6.1)

Data are presented as counts or mean ± standard deviation; data in parentheses are percentages.

Fig. 1. Chest CT findings of COVID-19 pneumonia, acute alveolar insult pattern.

A. Consolidation.

B. Mixed pattern with crazy-paving appearance.



served (Fig. 1). In the later hospital and discharge groups, band opacity, perilobular patterns, small nodular consolidation, and thin curvilinear opacity were observed more frequently (Fig. 2). In the follow-up group, pure GGO, remnant small nodular consolidation, or thin curvilinear opacity were predominant findings (Figs. 3, 4). Peribronchovascular and peripheral subpleural areas were primarily involved. Diffuse ($n = 5$) or anterior-posterior gradient involvement ($n = 2$) was observed in clinically severe patients (Table 2). Well-defined centrilobular nodules were observed on six CT scans of patients with known pulmonary TB, and no serial changes of the lesions were observed on serial CT scans. The lesions were considered bronchiolitis due to previous pulmonary TB, not COVID-19 pneumonia. Pleural effusion was noticed in six patients with lung abscess or congestive heart failure, and it is not clear whether the pleural effusion was caused by COVID-19 pneumonia.

The AAI pattern (87%) was predominantly observed in CT scans of the early hospital period group, and the OP pattern was predominant (47.2%) in the later hospital period group. The resulting pattern was predominant in the discharge and follow-up groups (47.2% and 84.8%, respectively) (Table 3). The difference in proportions for AAI pattern, OP pattern, or resolving pattern with time progression was statistically significant ($p < 0.001$, Pearson's chi-square test). No statistically significant association was observed between the patterns and disease severity ($p = 0.055$, Fisher's exact test). The study noticed no obvious fibrous changes in the lesions on follow-up CT scans.

DISCUSSION

Recently, several studies have reported temporal changes in CT findings for COVID-19 pneumonia that GGO is the earliest chest CT finding, followed by crazy-paving appearance, mixed pattern, or consolidation on earlier illness period, linear opacity, or reverse halo sign on later illness period, and residual lung abnormality of GGO during the recovery period (6, 12, 13). The authors have suggested an exudative phase followed by an organizing nature period.

Fig. 2. Chest CT findings of COVID-19 pneumonia, organizing pneumonia pattern.

- A. Perilobular consolidation.
- B. Band opacity.
- C. Small nodular consolidation with ground-glass opacity.



A clinical report also noted lung edema, which is a manifestation of ALI, and acute alveolar damage (AAD), may progress to clinically ARDS, as a central pathophysiological component of COVID-19 pneumonia (14).

Fig. 3. Serial changes of CT findings in a 59-year-old male patient with COVID-19 pneumonia.

- A.** On early hospital period (day 5), subpleural GGO with inter- and intraseptal thickening (crazy-paving appearance) with consolidations are shown.
 - B.** At discharge (day 26), partial resolution with perilobular consolidation, and small nodular consolidations are shown.
 - C.** On 1st follow-up (day 52), continued resolution with perilobular GGO, remnant small nodular consolidations, and curvilinear opacity are shown.
 - D.** On 2nd follow-up (day 85), resolved with subtle pure GGO is resolved.
- GGO = ground-glass opacity

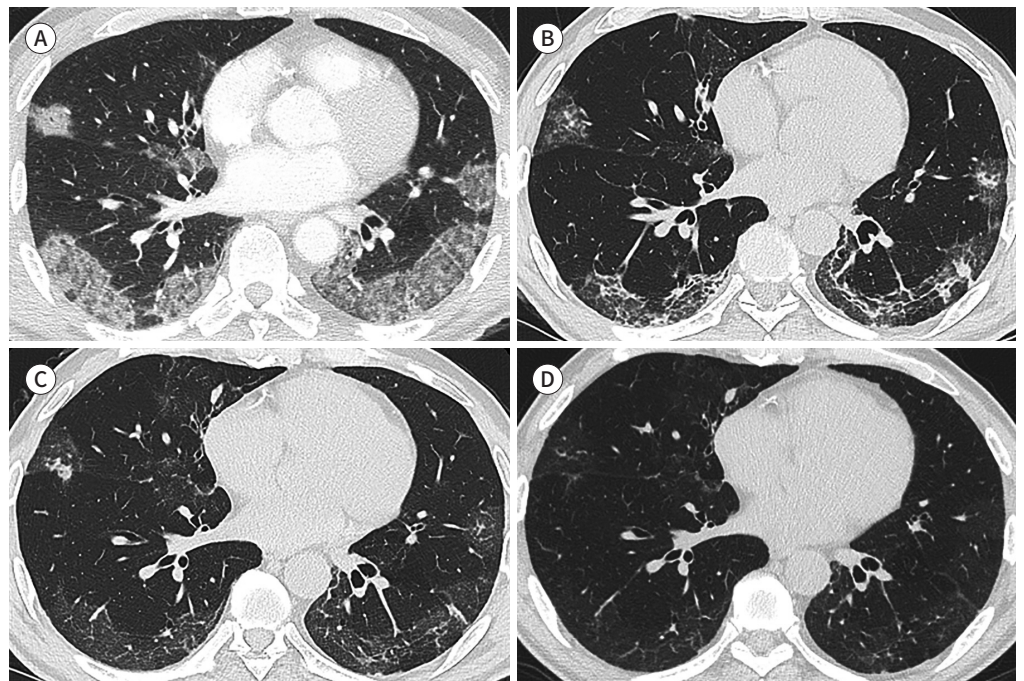


Fig. 4. Serial changes of CT findings in a 64-year-old female patient with COVID-19 pneumonia.

- A.** On early hospital period (day 7), a lesion of subpleural consolidation is shown.
 - B.** On later hospital period (day 21), resolution of lesion with small nodular consolidation with GGO is shown.
 - C.** On follow-up (day 47), resolved with subtle pure GGO is resolved.
- GGO = ground-glass opacity



Table 2. Per-Group Analysis of Chest CT Findings

	Early Hospital Period Group (n = 23)	Later Hospital Period Group (n = 70)	Discharge Group (n = 108)	Follow-Up Group (n = 33)	p-Value
Days from symptoms onset to CT scan	5.5 ± 3.5	20.3 ± 7.1	33.3 ± 14.1	67.2 ± 14.3	
CT findings					
Normal	3 (13.0)	15 (21.4)	37 (34.2)	3 (9.1)	0.009
Pure GGO	6 (26.1)	5 (7.1)	14 (13.0)	21 (63.6)	<0.001
Crazy-paving appearance	7 (30.4)	1 (1.4)	1 (0.9)	0	<0.001
Mixed opacity	12 (52.2)	8 (11.4)	2 (1.9)	1 (3.0)	<0.001
Consolidation	10 (43.5)	10 (14.3)	0	0	<0.001
Air-bronchogram	5 (21.7)	7 (10.0)	0	0	<0.001
Band opacity	2 (8.7)	17 (24.3)	10 (9.3)	1 (3.0)	0.008
Perilobular consolidation	1 (4.3)	35 (50.0)	14 (13.0)	2 (6.1)	<0.001
Perilobular GGO	0	16 (22.9)	35 (32.4)	9 (27.3)	0.013
Small nodular consolidation	2 (8.7)	27 (38.6)	50 (46.3)	15 (45.5)	0.009
Thin curvilinear opacity	0	17 (24.3)	33 (30.6)	12 (36.4)	0.012
Centrilobular nodule	1 (4.3)	2 (2.9)	3 (2.8)	0	0.805
Pleural effusion	0	4 (5.7)	2 (1.9)	0	0.370
Location					
Peribronchovascular	9 (39.1)	26 (37.1)	30 (27.8)	10 (30.3)	0.510
Subpleural	15 (65.2)	42 (60.0)	48 (44.4)	21 (63.6)	0.061
Diffuse	3 (13.0)	2 (2.9)	0	0	0.033
Anterior-posterior gradient	1 (4.3)	1 (1.4)	1 (0.9)	1 (3.0)	0.358
Number of involving lobe	3.1 ± 1.9	2.9 ± 1.9	2.0 ± 2.1	3.4 ± 2.1	

Data were presented as counts or mean ± standard deviation. Data in parentheses are the percentages; Pearson's chi-square test or Fisher's exact test was used to evaluate differences among nominal variables. *p* values < 0.05 were considered as statistically significant.

GGO = ground-glass opacity

Table 3. Per-Group Analysis of Chest CT Patterns

	Early Hospital Period Group (n = 23)	Later Hospital Period Group (n = 70)	Discharge Group (n = 108)	Follow-Up Group (n = 33)
Normal	3 (13.0)	15 (21.4)	37 (34.3)	3 (9.1)
AAI pattern	20 (87.0)	6 (8.6)	0	0
Transitional pattern	0	7 (10.0)	0	0
OP pattern	0	32 (45.7)	20 (18.5)	2 (6.1)
Resolving pattern	0	10 (14.3)	51 (47.2)	28 (84.8)

Data are presented as counts, data in parentheses are the percentage.

AAI = acute alveolar insult, OP = organizing pneumonia

Tian et al. (2) reported pathological findings of the lung in the early stage of COVID-19 patients. In their report, the specimens showed edema, exudate, and focal pneumocyte hyperplasia with patchy inflammatory cellular infiltration, without hyaline membranes as very early findings of COVID-19 pneumonia, indicating DAD. The authors also reported a pathological study of COVID-19 pneumonia by postmortem biopsy, in which the main findings are

DAD with hyaline membrane formation, and organization with fibrin plugs in the alveolar wall is evident, demonstrating a sequential change in COVID-19 pneumonia (2, 15).

The majority of COVID-19 patients demonstrated pneumonia as presenting illness. Therefore, the lung is considered the major target organ of the virus. Recently, angiotensin-converting enzyme 2 (ACE 2) protein has been proposed as the receptor for viral spike protein, which gives the route into the lung to the virus. ACE 2 protein is mainly expressed in type II alveolar epithelial cells (pneumocytes) and is barely present in other lung cells, such as bronchial epithelial cells and endothelial cells (16). Therefore, alveoli are the main target lung structures for SARS-CoV-2.

Among the various causes of lung injury, virus has been considered as the etiology of ALI (17). ALI commonly shows pathological DAD. DAD is a histologic term that demonstrates AAD of all layers, including alveolar epithelial cells, basement membranes, and capillary endothelial cells. AAD followed by OP has well-defined histologic findings as sequential changes of lung injury. Lung repair following acute injury showed acute damage of alveolar epithelial cells, basement membranes, or capillary endothelial cells, resulting in alveolar collapse, protein-rich exudate leakage, and hyaline membrane formation, followed by organization of exudate materials, and fibrin plug formation in the alveolar wall (18).

In the context of radiologic findings of AAD and OP, Obadina et al. have demonstrated that consolidation, GGO, and crazy-paving pattern are CT findings of acute, or exudate phase of AAD during, which showed during first week after the initial insult. The organizing phase of AAD occurs after 1–2 weeks (5). The CT findings correlated with OP have also been documented as multifocal peripheral, and bronchocentric consolidation, acinar type nodules, perilobular opacities, band-like opacity, reversed halo opacity, and crazy-paving appearance (7, 8).

In this study, we observed that the early stage of COVID-19 pneumonia showed CT patterns of AAI, followed by patterns of OP. This finding showed good correlation with previous concepts of ALI followed by organization, and with documented radiologic findings for AAD and OP. Interestingly, ill-defined small nodular consolidation somewhat resembling tree-in-bud pattern was frequently observed in the present study. The nodules were noticed in areas where consolidations had been noticed previously. In addition, these lesions were observed predominantly in CT scans of patients with organizing and resolving states. This nodular lesion may be a remnant consolidation mainly involving a small acinar. Yoon et al. reported a single nodular lesion as one of the CT findings of COVID-19 pneumonia that showed a 2.3-cm nodular opacity with a reversed halo appearance (19). Moreover, a small GGO nodule progressing to GGO lesion at the initial stage of COVID-19 pneumonia was reported in a case report (20). Considering that acinar type nodules have been demonstrated as one of the CT findings for OP in many articles, it could be considered as an acinar type nodule, or remnant consolidation with some organization (7, 8, 21-24). Therefore, we suppose that it may show organizing state of COVID-19 pneumonia.

Our study has several limitations. First, we did not acquire tissue samples for pathologic confirmation, but biopsy was very difficult for COVID-19 patients, considering transmission of the virus. Second, there was bias for patient selection since our center was designated as the hospital for patients with moderate severity according to the government guidelines.

In conclusion, we have analyzed serial CT scans of COVID-19 patients that demonstrated a spectrum showing ALI and repair. Various CT findings from COVID-19 pneumonia could be explained by AAD followed by OP without the development of fibrosis.

Author Contributions

Conceptualization, K.U.R.; data curation, K.U.R.; formal analysis, K.U.R.; investigation, K.Y.S.; methodology, K.U.R.; project administration, K.U.R.; resources, K.Y.S.; supervision, K.Y.H.; validation, K.Y.H.; visualization, K.Y.S.; writing—original draft, K.U.R.; writing—review & editing, K.U.R.

Conflicts of Interest

The authors have no potential conflicts of interest to disclose.

Funding

This study was supported by a research grant from Daegu Medical Association COVID-19 scientific committee.

Acknowledgments

The authors would like to acknowledge Jung Ju Shin for assistance in improving the English usage in this manuscript.

REFERENCES

1. Zhu N, Zhang D, Wang W, Li X, Yang B, Song J, et al. A novel coronavirus from patients with pneumonia in China, 2019. *N Engl J Med* 2020;382:727-733
2. Tian S, Xiong Y, Liu H, Niu L, Guo J, Liao M, et al. Pathological study of the 2019 novel coronavirus disease (COVID-19) through postmortem core biopsies. *Mod Pathol* 2020;33:1007-1014
3. Zhang H, Zhou P, Wei Y, Yue H, Wang Y, Hu M, et al. Histopathologic changes and SARS-CoV-2 immunostaining in the lung of a patient with COVID-19. *Ann Intern Med* 2020;172:629-632
4. Hong KH, Lee SW, Kim TS, Huh HJ, Lee J, Kim SY, et al. Guidelines for laboratory diagnosis of coronavirus disease 2019 (COVID-19) in Korea. *Ann Lab Med* 2020;40:351-360
5. Obadina ET, Torrealba JM, Kanne JP. Acute pulmonary injury: high-resolution CT and histopathological spectrum. *Br J Radiol* 2013;86:20120614
6. Wang Y, Dong C, Hu Y, Li C, Ren Q, Zhang X, et al. Temporal changes of CT findings in 90 patients with COVID-19 pneumonia: a longitudinal study. *Radiology* 2020;296:E55-E64
7. Robertson BJ, Hansell DM. Organizing pneumonia: a kaleidoscope of concepts and morphologies. *Eur Radiol* 2011;21:2244-2254
8. Baque-Juston M, Pellegrin A, Leroy S, Marquette CH, Padovani B. Organizing pneumonia: what is it? A conceptual approach and pictorial review. *Diagn Interv Imaging* 2014;95:771-777
9. Lee SE, Kim YS. Clinical and radiological findings of coronavirus disease 2019 pneumonia: 51 adult patients from a single center in Daegu, South Korea. *J Korean Soc Radiol* 2020;81:591-603
10. Korea Centers for Disease Control and Prevention. The updates of COVID-19 in the Republic of Korea. Available at: <https://www.cdc.go.kr/board/board.es?mid=a20501000000&bid=0015>. Accessed Mar 18, 2020
11. Liu KC, Xu P, Lv WF, Qiu XH, Yao JL, Gu JF, et al. CT manifestations of coronavirus disease-2019: a retrospective analysis of 73 cases by disease severity. *Eur J Radiol* 2020;126:108941
12. Pan F, Ye T, Sun P, Gui S, Liang B, Li L, et al. Time course of lung changes on chest CT during recovery from 2019 novel coronavirus (COVID-19) pneumonia. *Radiology* 2020;295:715-721
13. Bernheim A, Mei X, Huang M, Yang Y, Fayad ZA, Zhang N, et al. Chest CT findings in coronavirus disease-19 (COVID-19): relationship to duration of infection. *Radiology* 2020;295:200463
14. Li L, Huang Q, Wang DC, Ingbar DH, Wang X. Acute lung injury in patients with COVID-19 infection. *Clin Transl Med* 2020;10:20-27
15. Tian S, Hu W, Niu L, Liu H, Xu H, Xiao SY. Pulmonary pathology of early-phase 2019 novel coronavirus (COVID-19) pneumonia in two patients with lung cancer. *J Thorac Oncol* 2020;15:700-704
16. Zou X, Chen K, Zou J, Han P, Hao J, Han Z. Single-cell RNA-seq data analysis on the receptor ACE2 expres-

sion reveals the potential risk of different human organs vulnerable to 2019-nCoV infection. *Front Med* 2020;14:185-192

17. Gralinski LE, Bankhead A 3rd, Jeng S, Menachery VD, Proll S, Belisle SE, et al. Mechanisms of severe acute respiratory syndrome coronavirus-induced acute lung injury. *mBio* 2013;4:e00271-13
18. Kligerman SJ, Franks TJ, Galvin JR. From the radiologic pathology archives: organization and fibrosis as a response to lung injury in diffuse alveolar damage, organizing pneumonia, and acute fibrinous and organizing pneumonia. *Radiographics* 2013;33:1951-1975
19. Yoon SH, Lee KH, Kim JY, Lee YK, Ko H, Kim KH, et al. Chest radiographic and CT findings of the 2019 novel coronavirus disease (COVID-19): analysis of nine patients treated in Korea. *Korean J Radiol* 2020;21:494-500
20. Xia T, Li J, Gao J, Xu X. Small solitary ground-glass nodule on CT as an initial manifestation of coronavirus disease 2019 (COVID-19) pneumonia. *Korean J Radiol* 2020;21:545-549
21. Müller NL, Miller RR. Diseases of the bronchioles: CT and histopathologic findings. *Radiology* 1995;196:3-12
22. Lee KS, Kim EA. High-resolution CT of alveolar filling disorders. *Radiol Clin North Am* 2001;39:1211-1230
23. Hochegger B, Langer FW, Irion K, Souza A, Moreira J, Baldisserotto M, et al. Pulmonary acinus: understanding the computed tomography findings from an acinar perspective. *Lung* 2019;197:259-265
24. Bots EM, den Bakker MA, Wijsenbeek MS, van den Toorn LM, van den Blink B. "Tree in bud" attributable to organising pneumonia. *Thorax* 2013;68:399-400

COVID-19 폐렴의 다양한 CT 영상 소견: 급성 폐포 손상과 기질화 폐렴

김윤수 · 강웅래* · 김영환

목적 증상이 있는 123명의 coronavirus disease 2019 (이하 COVID-19) 환자에서 흉부 CT 병변의 소견과 일련의 변화를 분석하였다.

대상과 방법 2020년 2월 19일부터 4월 7일까지 총 123명의 COVID-19 환자(남성, 44명; 여성, 79명; 평균 연령 59.2 ± 18.6)를 후향적으로 연구하였다. 총 234개의 CT 스캔을 검토하여 패턴[급성 폐포 손상(acute alveolar insult) 패턴: 간유리음영, 돌조각보도모양, 혼합된 패턴, 또는 폐경화; 기질화 폐렴(organizing pneumonia) 패턴: 소엽주위 패턴, 띠 음영, 곡선형 음영, 역달무리 음영, 또는 소결절경화; 호전형 패턴: 순수 간유리음영, 잔존 곡선형 음영, 또는 소결절경화]과 폐 이상의 연속적인 변화를 분석하였다. 피어슨 카이 제곱 검정과 피셔의 정확 검정을 사용하여 시간 경과에 따른 급성 폐포 손상 패턴, 기질화 폐렴 패턴, 호전형 패턴의 비율을 비교하고, 패턴과 질병 심각도 간의 연관성을 분석하였다.

결과 초기 입원군(증상 발병 후 0~10일)의 CT 패턴은 급성 폐포 손상 패턴(87%)이 가장 많았고, 후기 입원군(10일 이상)에서는 기질화 폐렴 패턴(45.7%), 퇴원군(퇴원 시 및 퇴원 후)에서는 호전형 패턴(47.2%; 84.8%)이 가장 많았다. 시간 경과에 따른 우세한 CT 패턴에 대한 비율의 차이는 통계적으로 유의하였다($p < 0.001$, 피어슨 카이 제곱 검정). 패턴과 질병 중증도 간에 통계적으로 유의한 연관성은 발견되지 않았다($p = 0.055$, 피셔의 정확 검정). 후속 CT 스캔에서 병변의 섬유화는 관찰되지 않았다.

결론 COVID-19 환자의 연속적 CT 스캔은 COVID 폐렴의 폐 손상 및 복구의 단계로서 다양한 CT 영상 소견을 보여주었다.

대구가톨릭대학교 의과대학 대구가톨릭대학교병원 영상의학과